Journal of Thermal Analysis and Calorimetry (2023) 148:5943–5956
https://doi.org/10.1007/s10973-023-12158-5

Hexagonal boron nitride-loaded macroporous foams as frameworks for development of n-eicosane-based composite phase-change materials

Hatice Hande Mert[1] · Esra Bilgin Simsek[1] · Zeynep Balta[1] · Mehmet Selçuk Mert[2]

Received: 22 August 2022 / Accepted: 25 March 2023 / Published online: 11 April 2023

Abstract
The development of a new composite phase change material (PCM) was accomplished by using n-eicosane, which was belonging to the paraffins. For this goal, hexagonal boron nitride (h-BN)-loaded macroporous foams were synthesized by emulsion-templating method. The resulting foams were used as supporting materials in the preparation of n-eicosane-based composite PCMs that have improved thermal conduction property. The h-BN was synthesized as additive with the aim of thermal conductivity enhancement, and the porous supporting materials were obtained by polymerization of high internal phase emulsions (HIPEs) at various loadings of h-BN nano-fillers (0, 1, 5 and 9 mass/%). The h-BN, h-BN-loaded macroporous polyHIPE foams (MPFs) and composite PCMs were fully characterized by SEM, BET, FT-IR, TG and DSC analysis techniques. Furthermore, leak-proof and phase-change properties of composite PCMs were tested in addition to investigation of thermal behavior with a thermal performance test. The highest thermal energy storage (TES) capacity among the produced n-eicosane-based h-BN-loaded MPFs was belonging to 1 mass/% h-BN-loaded composite PCM having 79 J g^{-1} latent heat of melting and 38.79 °C melting temperature; the composite was also comprised of the supporting matrix with highest specific surface area. Based on the results, thermally conduction enhanced n-eicosane-based composite PCMs are promising materials for thermal management applications, such as electronic package and electronics cooling, with thanks to high latent heats (range between 72.2 and 79 J g^{-1}) and convenient phase transition temperature as well as anti-leakage property.

Keywords n-eicosane · Hexagonal boron nitride · polyHIPE · Composite phase-change material · Thermal energy storage

Introduction

Introducing an increment of energy demand in relation to day by day, growth population and industrialization and the safe energy supply are important issues of today for many countries in the global world. The dependence on fossil fuels in energy supplies both creates a constraint in terms of economic due to fluctuation in prices and causes global warming as a result of the accumulation of greenhouse gases in the atmosphere. In this respect, the use and progression of renewable energy sources are crucial in terms of overcoming the dependence on foreign energy supply and eliminating the environmental concerns as a result of reducing the usage of fossil fuels. Today, it is possible to achieve this goal with thermal energy storage (TES) technology built on phase-change materials (PCMs), and researchers began to concentrate this field together with increasing demand.

The PCMs are functional materials, which have the thermoregulating mission that can store or release latent heat at a certain temperature during phase change [1, 2]. During the heating process, phase transition of PCM at temperature above the melting temperature occurs, and PCM transforms from solid into the liquid state. PCMs have some defects such as low thermal conductivity and leakage during phase change. Thermal conductivity is an important property that indicates the heat transfer response of a material. Low thermal conductivity and leakage problem limit the use of PCMs as thermal energy storage material. Low thermal conductivity leads to reducing the heat transfer rate, and seepage during phase transition causes waste/loss of PCM

✉ Mehmet Selçuk Mert
msmert@yalova.edu.tr

[1] Chemical Engineering Department, Yalova University, 77200 Yalova, Turkey

[2] Energy Systems Engineering Department, Yalova University, 77200 Yalova, Turkey

in addition to serious damage to the equipment/storage unit/electronic device directly used [3]. At this point, limitation of PCM in a framework as a support material is crucial for effective use in thermal energy storage applications [4]. In addition, low thermal conductivity increases the charge/discharge period of organic type PCM and limits the efficient use of latent heat storage capacity [5]. Paraffins as members of organic type of PCMs could be encapsulated in micro- or nano-sized with organic or inorganic shell for stabilization in liquid form and prevention against an external effect. Shape-stabilization of PCMs could be achieved in different ways such as micro- or nano-encapsulation within organic polymer or impregnation of the PCMs within a supporting matrix [6]. By the shape-stabilization process, it is possible to improve the structural, chemical and thermal stability of PCMs with various additives. The thermal properties of phase-change materials can be developed, and the heat storage/release rates can be increased by adding nano-sized solid particles such as metal particles, metal oxides, carbon nanotubes, carbon fiber, expanded graphite, graphene oxide, Al_2O_3, Ag, TiO_2 and MXene with high thermal conductivity [5, 7–10]. During the preparation of shape-stable composite materials, incorporation of nano-sized materials leads to improve the heat transfer rate of organic PCM due to acting as a catalyst thanks to their high surface area/volume ratio and excellent thermal conductivity.

Although graphene-based fillers have become prominent for improving low thermal conductivity of organic PCMs, other carbon-based materials, such as carbon nanotubes, carbon fibers, etc., have an increasing interest in recent years due to providing remarkable improvement in heat transfer rate [11]. Hexagonal boron nitride (h-BN) is a two-dimensional (2-D) nano-filler, which serves as an ideal material for thermal enhancement of PCM due to high thermal conductivity besides to have unique properties such as high mechanical hardness, chemical stability, flame retardant and high electrical insulation [11–14]. Moreover, boron nitride is used for developing thermally conductive polymer composites in recent years for especially thermal management of electronic devices [13, 15].

Until today, few researches were reported about developing PCM composites based on h-BN for thermal energy storage in the literature, which were mostly focused on usage of h-BN as a support material or filler for PCM. Fang et al. prepared paraffin wax-based composite PCMs loaded with h-BN nanosheets at different loadings and characterized their thermal properties [16]. Su et al. synthesized composite PCMs by using eutectic mixtures of n-octadecane/stearic acid as PCM and h-BN as filler and investigated thermal properties of composites [17]. In another work, Xie et al. prepared three types of h-BN nanosheets with different exfoliation degrees by hydrothermal exfoliation methods and used them as support materials for obtaining stearic acid-based composite PCM by vacuum impregnation method [18].

PolyHIPEs are emulsion-templated polymer foams, which prepared by polymerization of high internal phase emulsions. In recent years, the development of polyHIPE as polymeric support material for PCMs has an increasing interest due to unique structure composed of cavities with interconnected hierarchical pores and high absorbance capacity [19–24]. Even though polymeric support materials provide shape-stabilization of PCM, it would cause to decrease of thermal conductivity and heat transfer rate throughout heat charging and discharging processes in thermal energy storage systems due to the limitation of PCM in a polymeric framework. In this respect, novel polyHIPE composites can be developed as support material not only for the purpose of the providing shape-stabilization of PCM but also improving thermal stability and heat transfer rate by introduction of highly conductive fillers to the support matrix.

In this study, as distinct from studies in the literature, novel h-BN-loaded macroporous heat conductive polymer composites with enhanced heat transfer performance were developed with the aim of using as support materials for preparing n-eicosane-based shape-stabilized composite PCMs for TES application in electronic devices. The service life, performance and durability are the main criteria for thermal management of electronic equipment, and this required design of polymer-based composite PCMs with improved thermal conduction. For this aim, n-eicosane was selected as PCM, which is widely used for cooling of electronic devices with thanks to its suitable melting temperature (34–37 °C) [4], while the nano-sized h-BN was used as a thermal enhancement additive for improvement of heat conduction of porous polymer matrix. The obtained composite PCMs, which can be promising composites for thermal management of electronic devices, were fully characterized for investigation of chemical, morphological and thermal properties.

Experimental

Materials

Styrene (purity 99%, Merck), divinylbenzene (purity 80%, Aldrich Chemistry), Span 80® (Aldrich Chemistry), n-eicosane (purity 99%, Alfa Aesar), $CaCl_2.6H_2O$ (purity 98%, Sigma-Aldrich) and potassium peroxodisulfate (purity ≥ 99.0%, ACS reagent) were employed as received. Boric acid (H_3BO_3, 99%) and melamine ($C_3N_6H_6$, 99%) were supplied from Merck. Ultrapure water was used during the synthesis of emulsion-templated polyHIPE frameworks.

Methods

Preparation of h-BN

Hexagonal boron nitride (h-BN) was produced by using boric acid (H_3BO_3) and melamine ($C_3N_6H_6$) as precursors as described in the previous work [25]. In a typical experimental run, H_3BO_3 and $C_3N_6H_6$ with 1:1 molar ratio were mixed in deionized water under stirring at 90 ºC for 30 min. After 24 h stirring at room temperature, a white crystalline powder was formed, which was filtered and dried. Then, the white precursors were put into a ceramic boat and then heated in a tube furnace at 900 ºC for 3 h under nitrogen/hydrogen (5% hydrogen) gas flow. The resultant sample was coded as h-BN.

Synthesis of h-BN-loaded macroporous PolyHIPE foams (MPFs)

A series of h-BN-loaded MPFs were synthesized from high internal phase emulsions (HIPEs) by emulsion-templating method. The total emulsion comprised of two phases as monomer phase (20 vol. %) and internal phase (80 vol. %). The monomer phase consisting of styrene (90 vol %), divinyl benzene (10 vol %), Span 80® (3 mL) and h-BN (at varying mass/% with respect to monomer phase) was stirred vigorously at room temperature for 30 min. The internal phase consisting of ultrapure water, $CaCl_2.6H_2O$ (1 mass/%) and potassium peroxodisulfate (0.25 mass/%) was dropped into monomer phase and stirred mechanically at 500 rpm. The obtained HIPEs were polymerized in a vacuum oven at 60 °C and then purified by Soxhlet extraction. The obtained h-BN-loaded MPFs are dried in a vacuum oven and named according to the h-BN mass percent as given in Table 1.

Preparation of n-eicosane-based composite phase-change materials

The h-BN-loaded MPFs were employed as supporting matrix for preparation of n-eicosane-based composite PCMs. The macroporous monoliths were ground into powder by crushing in a mortar. N-eicosane was melted in an ultrasonic bath at 45 °C, and then, 100 mL of ethanol was added. The PCM solution was stirred at 45 °C for 30 min. The homogeneous PCM solution was poured onto h-BN-loaded MPF and then placed into an ultrasonic bath. After ultrasonically inducing process at 45 °C, the solution stirred vigorously at 45 °C for 24 h. At the end of the stirring process, ethanol was evaporated in a vacuum oven at 80 °C, and dried composite PCMs were obtained. During the preparation process, mass fraction of n-eicosane was fixed 62.5 mass/% for all composites. N-eicosane-based composite PCMs were named as "*MPF-hBN-x-EC*". *x* was denoted as h-BN mass percent presented in composite PCM.

Table 1 Composition of h-BN-loaded MPFs

polyHIPE foams	h-BN[a]/ mass/%
MPF	0
MPF-hBN-1	1
MPF-hBN-5	5
MPF-hBN-9	9

[a]According to the total amount of monomer phase

Characterization

Scanning electron microscopy (SEM, Philips XL30 ESEM-FEG/EDAX) was utilized to investigate the surface morphology of raw h-BN material. The Fourier transfer infrared spectroscopy (FT-IR) data were obtained on Perkin–Elmer Spectrum One by using an attenuated total reflectance indenter. The surface area of raw h-BN was determined from the nitrogen adsorption and desorption isotherms using a Quadrasorb SI-MP analyzer at 77 K. Morphology of MPF, h-BN-loaded MPFs and n-eicosane-based composite PCMs were investigated by using scanning electron microscope (FEI, Quanta FEG 250). Specific surface area values of h-BN-loaded MPFs were determined by surface area and porosimetry analyzer (Micromeritics Gemini VII 2390t) based on the Brunauer–Emmet–Teller (BET) adsorption model, while the thermal stabilities of foams were examined at temperature range of 25–600 °C by Seiko, TG/DTA 6300 system with 10 ºC min^{-1} heating rate under inert nitrogen atmosphere condition. Differential scanning calorimetry (DSC) analysis was conducted by using Seiko, DSC 7020 instrument for the determination of phase transition temperatures and enthalpies of n-eicosane and composite PCMs under inert nitrogen atmosphere with 5 ºC min^{-1} heating rate from − 20 to 80 °C. The chemical structure of n-eicosane, h-BN-loaded MPF and n-eicosane-based composite PCM were examined by FT-IR spectroscopy (Perkin–Elmer, Spectrum 100, FT-IR spectrophotometer) at the wavelength range from 500 to 4000 cm^{-1}. Thermal cycling test was carried out with Ruicheng MTC3200 Thermal Cycler Instrument at the range of 5 ºC to 50 ºC by performing 100 heating–cooling cycles.

Results and discussion

Characterization of h-BN

The morphological and chemical characterization of the prepared h-BN was obtained by SEM and FT-IR analyses,

respectively. The SEM images of h-BN used as thermally conductive loading material in porous-supporting polymeric foams are given in Fig. 1. As observed in Fig. 1, h-BN illustrated fiber-like uniform morphology in accordance with the literature [12]. The approximate diameters of h-BN fibers determined from SEM images were 0.3–0.5 µm. Moreover, BET surface area of the synthesized h-BN fibers was found to be a quite high value as 1019 $m^2 g^{-1}$.

The chemical structure of h-BN fibers was investigated by FT-IR analysis, and the obtained spectrum is presented in Fig. 2. The characteristic absorption bands observed at 1500–1300 cm^{-1} and around 800 cm^{-1} are due to stretching vibration of B–N (in-plane) and bending vibration of B–N, respectively [12, 18, 26]. The broad peak seen at 3500–3000 cm^{-1} belongs to the stretching vibrations of –OH groups of absorbed moisture on the fibers.

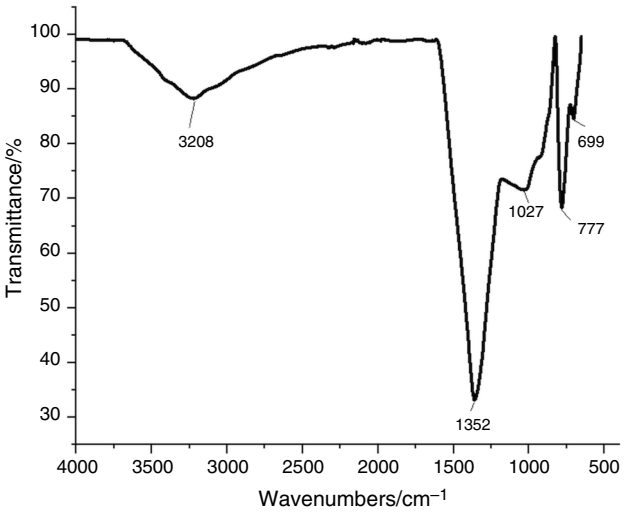

Fig. 2 FT-IR spectrum of the synthesized h-BN

Morphological and thermal characterization of h-BN-loaded MPFs

Morphological characterization of MPF and h-BN-loaded MPFs were investigated through SEM analysis, and the obtained views are demonstrated in Fig. 3. The pore structure of polyHIPE structure is a reflection of emulsion droplet size, which aroused depending on the maintenance of the emulsion stabilization process during the polymerization [27]. In this respect, emulsifier amount and particles involved in HIPEs are crucial for emulsion stabilization. As presented in Fig. 3, the samples were displayed open-cellular morphology as consistent with familiar polyHIPE structure. It can be seen from Fig. 3b and c, h-BN nanoparticles located on polymer matrix without any collapse of pore structure.

On the other hand, influence of nanoparticle loading amount on pore morphology was clearly noticed from Fig. 3e, which was the SEM image of 9 mass/% h-BN-loaded MPF. This differentiation in morphology is a sign of the beginning of reduction in emulsion stability due to increasing the amount of nanoparticle. Accordingly, it could be concluded that h-BN loading upper than 9 mass/% might lead to possible phase inversion. Moreover, the apparent effect of the nanoparticle amount on morphological properties could also be seen from Table 2, which gives specific surface area values of prepared porous material. It can be noticed from the specific surface area values of MPF and h-BN-loaded MPFs; the surface area values were increased at first and then decreased by loading h-BN nanoparticle due to changing emulsion stability and pore morphology.h-BN fiber distribution on polymer matrix was also investigated by EDX and elemental mapping analysis (with ZEISS EVO LS10 SEM/EDX instrument). EDX elemental mapping images and EDX spectrum of the MPF-hBN-9 composite are given in Fig. 4. As can be seen results presented in Fig. 4, C and O elements are related to polystyrene-divinylbenzene polymer matrix and possible surfactant residual in matrix, respectively. Moreover, the presence and homogeneous distribution of B and N elements confirmed the existence of h-BN particles on the surface of polymer composite material.

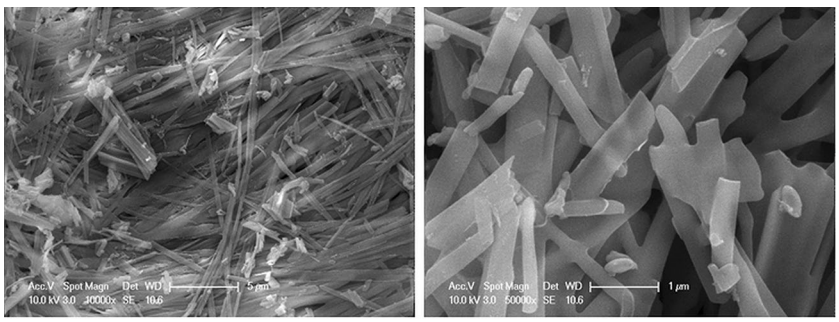

Fig. 1 SEM images of the synthesized h-BN

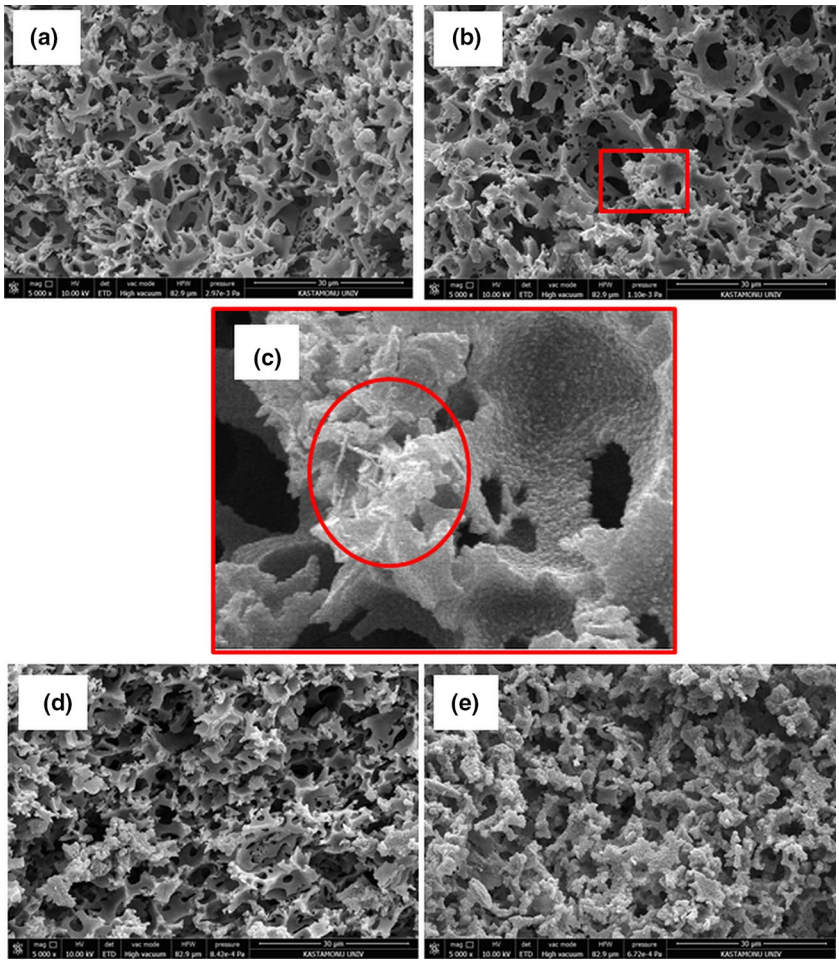

Fig. 3 SEM images of h-BN-loaded MPFs: **a** MPF, **b** MPF-hBN-1, **c** zoom view of MPF-hBN-1, **d** MPF-hBN-5 and **e** MPF-hBN-9

Table 2 Specific surface area of h-BN-loaded MPFs

Sample	δ_{BET} /m^2 g^{-1}
MPF	3.77
MPF-hBN-1	8.89
MPF-hBN-5	7.46
MPF-hBN-9	2.92

Thermal properties of prepared h-BN-loaded MPFs were investigated by TG analysis. TGA curves of samples are given in Fig. 5, and the corresponding data are presented in Table 3. In Table 3, Td_{10} and Td_{50} state that initial and midpoint degradation temperatures, respectively, corresponding to the temperatures at which sample lost 10 and 50% of its mass. Moreover, T_{max} is the temperature, which corresponding to the maximum decomposition rate (V_{max}) is determined. Thermal degradation manner could be evaluated as closely related to the nanoparticle loading amount and the homogeneous distribution of nanoparticles in the polymer matrix. Also, pore morphology depending on emulsion stability can be also stated as an effective parameter on thermal stability of polyHIPE foam. According to Table 3, the positive contribution of presence of h-BN nanoparticles in terms of thermal stability could be obviously seen from the values of Td_{50} as compared to MPF without h-BN. The highest Td_{10} and Td_{50} values were found to be for MPF-hBN-5, which has also the highest T_{max} at corresponding V_{max}. On the other hand, a decrease was found at Td_{10} and Td_{50} values for MPF-hBN-9, which could be attributed to varying pore morphology based on the emulsion stability.

Characterization of n-eicosane-based composite phase-change materials

The phase transition temperatures (onset, peak and endset values) and latent heats of n-eicosane and composite PCMs during heating and cooling period were determined via DSC analysis. The obtained curves of the samples are presented in Fig. 6, and corresponding data are given in Table 4. As seen from Fig. 6, the presence of melting and crystallization peaks belong to composites confirmed that incorporation of n-eicosane into the MPFs. In addition, phase-change transitions of composites showed a similar trend to n-eicosane,

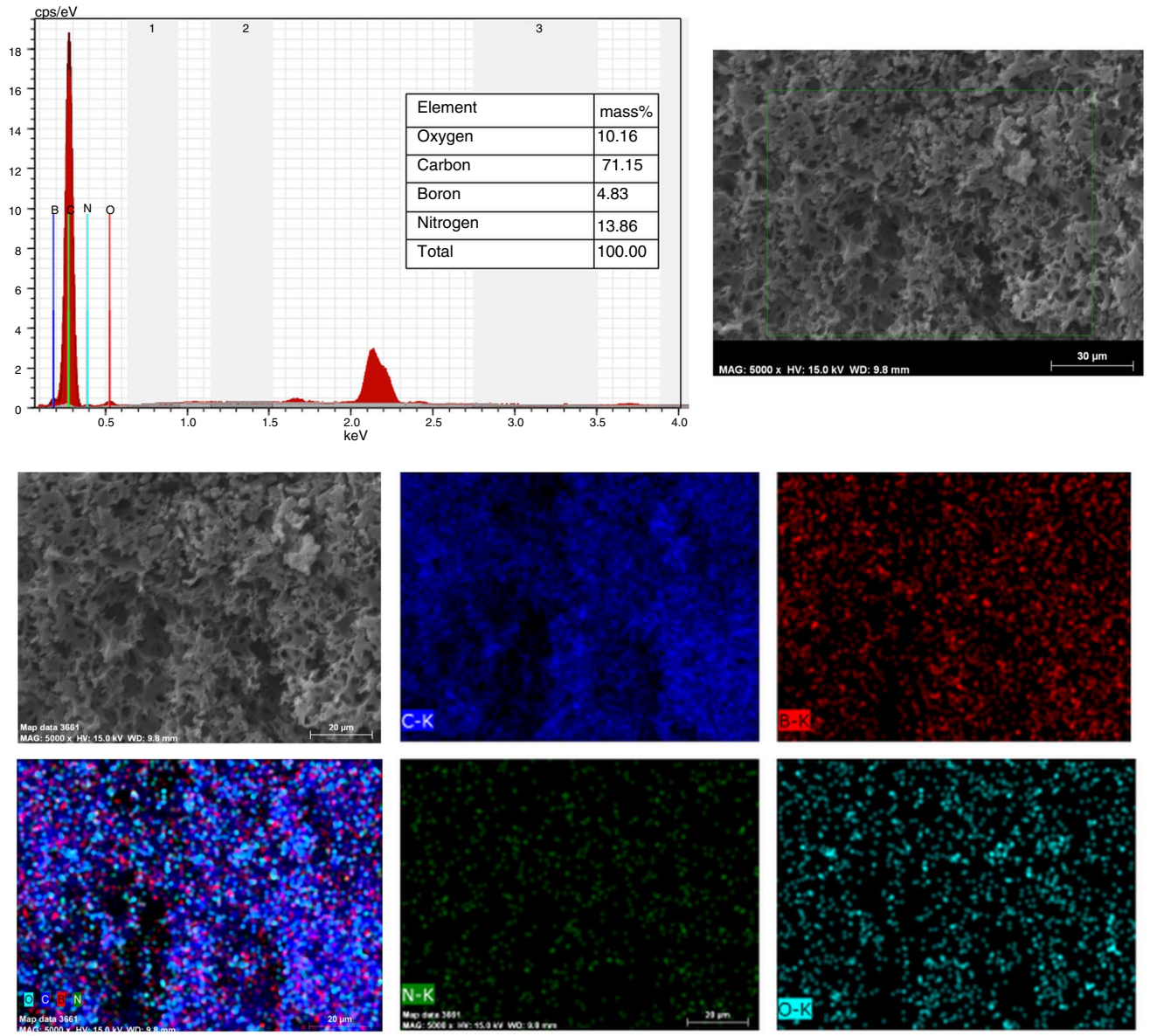

Fig. 4 EDX elemental mapping images and EDX spectrum of MPF-hBN-9 composite

which affirms that no chemical reaction happened between n-eicosane and polymeric support matrix. The onset melting and crystallization temperature are determined to be 33.82 and 34.02 °C for the n-eicosane and varying between 33.97 and 34.85 °C and 34.09–34.34 C for composite PCMs, respectively. The latent heats of melting and crystallization were found to be 133 and 139 J g^{-1} for the n-eicosane, while latent heats measured for composites as ranging between 72.20 and 79.00 J g^{-1} for melting and 68.50–74.50 J g^{-1} for crystallization. The observed slight shifts of melting and crystallization temperature values and decreased latent heats for composite PCMs as comparing with unrestricted PCM are expected results due to the limitation of n-eicosane into a support matrix.

The evaluation of thermal energy storage performance of obtained composite PCMs was performed by calculation of the incorporation ratio (R), incorporation efficiency (E) and thermal storage capability (η) according to the following equations [28, 29]:

$$R = \frac{\Delta H_{\mathrm{m,\,Composite\,PCM}}}{\Delta H_{\mathrm{m,PCM}}} \times 100\% \quad (1)$$

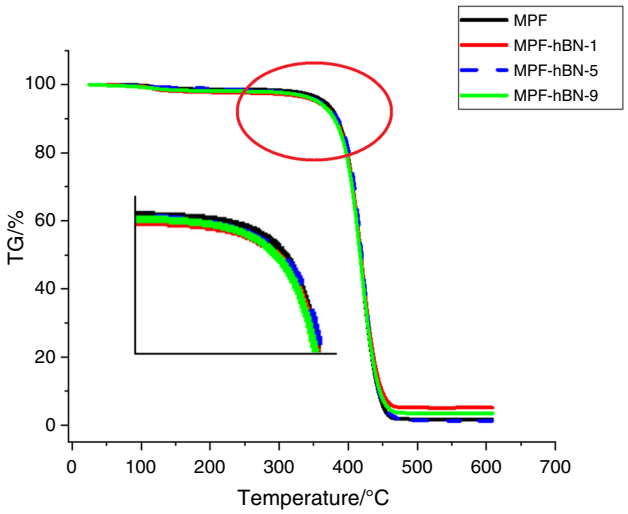

Fig. 5 TGA curves of h-BN-loaded MPFs

Table 3 TGA results of h-BN-loaded MPFs

Sample	T_{d10}/°C	T_{d50}/°C	V_{max}/% min^{-1}, T_{max}/°C
MPF	384.1	417.3	20.70 420.4
MPF-hBN-1	380.9	418.2	19.49 420.2
MPF-hBN-5	384.8	419.4	22.10 421.9
MPF-hBN-9	379.8	417.3	19.85 420.3

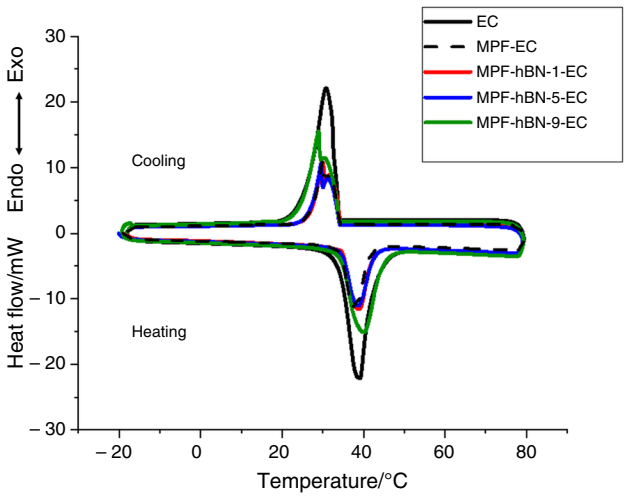

Fig. 6 DSC curves of n-eicosane-based composite PCMs

$$E = \frac{\Delta H_{\mathrm{m,\,Composite\,PCM}} + \Delta H_{\mathrm{c,\,Composite\,PCM}}}{\Delta H_{\mathrm{m,\,PCM}} + \Delta H_{\mathrm{c,\,PCM}}} \times 100\% \quad (2)$$

$$\eta = \frac{E}{R} \times 100\% \quad (3)$$

where $\Delta H_{\mathrm{m,Composite\ PCM}}$ and $\Delta H_{\mathrm{c,Composite\ PCM}}$ denote the melting and crystallization latent heat of the composite PCMs, respectively, while $\Delta H_{\mathrm{m,PCM}}$ and $\Delta H_{\mathrm{c,PCM}}$ are the melting and crystallization latent heat of the n-eicosane.

As presented in Table 5, incorporation ratio of composite PCMs, which reflect n-eicosane loading amount was ranging between 54.28 and 59.39%. The highest incorporation ratio was found to be 59.39% belongs to MPF-hBN-1-EC, which has also a support matrix with highest surface area. Moreover, incorporation efficiency of composite PCMs is given in Table 5. The incorporation efficiency is more convenient characteristic than the incorporation ratio since it is based on both melting and crystallization process for interpretation of working efficiency of obtained composite PCMs. The calculated incorporation efficiency values by using latent heat values belonged to the heating and cooling period were varying between 53.70 and 58.58%. The similar propensity was observed for incorporation efficiency, and the highest value (58.58%) was obtained for MPF-hBN-1-EC. Also, the thermal storage capability (η) of composite PCMs was determined and found as higher than 97% for all composite PCMs, which is an indicator of the ability of PCM about storing latent heat in the composites during the thermal energy storage/release performance.

FT-IR analyses were performed for confirmation of chemical structure of specimens, and the obtained spectra belonging to n-eicosane, h-BN-loaded MPF and n-eicosane-based composite PCM are presented in Fig. 7. In the spectrum of n-eicosane (Fig. 7a), the characteristic peaks were observed at 2909 and 2847 cm^{-1}, which are because of the stretching vibrations of C-H groups. Moreover, the peaks aroused at 1468 and 715 cm^{-1} correspond to the deformation vibration of C-H groups and the in-plane rocking vibration of CH_2 groups, respectively. In the spectrum of h-BN-loaded MPF (Fig. 7b), the absorption bands seen at around 1695–1452 cm^{-1} and at around 755–696 cm^{-1} are ascribed to, respectively, the aromatic C=C and C-H bendings. In the spectrum of n-eicosane-based composite PCM (Fig. 7c), the characteristic peaks attributed to n-eicosane and h-BN-loaded MPF were still observed, and no new band was aroused. This result confirms that impregnation of n-eicosane into the composite matrix successfully and physical interaction between n-eicosane and composite matrix.

The impregnation of n-eicosane into the porous polymer framework was proved via SEM analysis. In Fig. 8,

Table 4 DSC data belonging to phase-change properties of n-eicosane and composite PCMs

Samples	Heating period				Cooling period			
	[a]T_{om}/°C	[b]T_{pm}/°C	[c]T_{em}/°C	[d]ΔH_m/J g^{-1}	[e]T_{oc}/°C	[f]T_{pc}/°C	[g]T_{ec}/°C	[h]ΔH_c/J g^{-1}
EC	33.82	39.14	43.45	133	34.02	30.78	24.53	− 129
MPF-EC	33.97	37.87	41.69	72.20	34.09	31.72	26.59	− 68.50
MPF-hBN-1-EC	34.85	38.79	42.47	79.00	34.34	31.54	26.65	− 74.50
MPF-hBN-5-EC	34.52	38.65	43.08	73.50	34.11	31.24	26.24	− 69.30
MPF-hBN-9-EC	34.39	40.02	45.15	77.10	34.00	30.44	23.81	− 71.60

[a]Onset melting temperature
[b]Peak melting temperature
[c]Endset melting temperature
[d]Latent heat of melting
[e]Onset crystallization temperature
[f]Peak crystallization temperature
[g]Endset crystallization temperature
[h]Latent heat of crystallization

Table 5 The incorporation ratio (R), incorporation efficiency (E) and thermal storage capability (η) of composite PCMs calculated using latent heat storage (LHS) data obtained from DSC curves

Samples	R/%	E/%	η/%
MPF-EC	54.28	53.70	98.93
MPF-hBN-1-EC	59.39	58.58	98.63
MPF-hBN-5-EC	55.26	54.50	98.62
MPF-hBN-9-EC	57.96	56.75	97.91

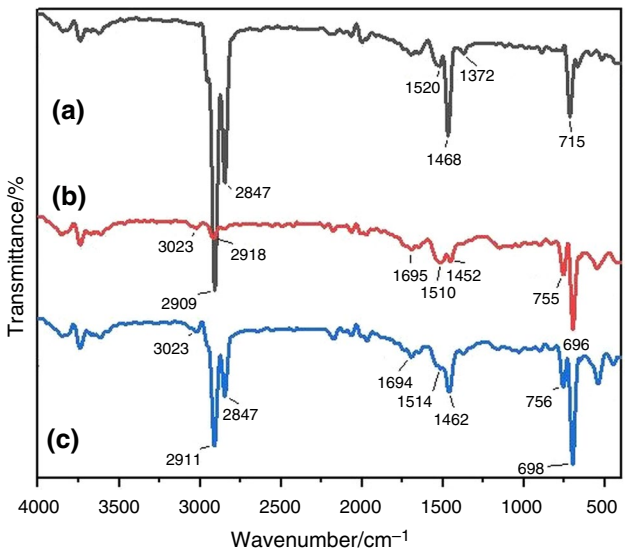

Fig. 7 FT-IR spectra of n-eicosane **a**, h-BN-loaded MPF (MPF-hBN-9) **b** and n-eicosane-based composite PCM (MPF-hBN-9-EC) **c**

SEM images of MPF and h-BN-loaded MPFs after the impregnation of n-eicosane were presented. As compared to SEM images given in Fig. 3, the coarse oily bulk layers partially or completely covered the cavities were monitored, which can be attributed to the presence of PCM.

Testing leak-proof properties of composite PCMs

A leakage test was carried out in a preheated vacuum oven for n-eicosane-based composite PCMs. N-eicosane and the composite samples placed on the filter papers and then kept in a vacuum oven at 50 °C for 1 h. At the end of the heating period, samples were taken out from the oven and stayed at room temperature for observing of any oily spot on filter paper. The photographs of filter papers that belonged to before and after the leakage test were taken and are depicted in Fig. 9. There was no observed any oil stain on filter papers for composite PCMs. On the other hand, solid EC disappeared due to melting after heating, and oily gray shades were observed on first filter paper. It is evident that from the Fig. 9, all composite PCMs containing n-eicosane displayed leak-resistive property.

Monitoring of thermal conduction performance and phase transition properties of composite PCMs

In this section, the performance of h-BN-loaded MPFs in terms of thermal conduction property and the phase transition behaviors of the obtained composite PCMs were investigated. For these purposes, two different scenarios

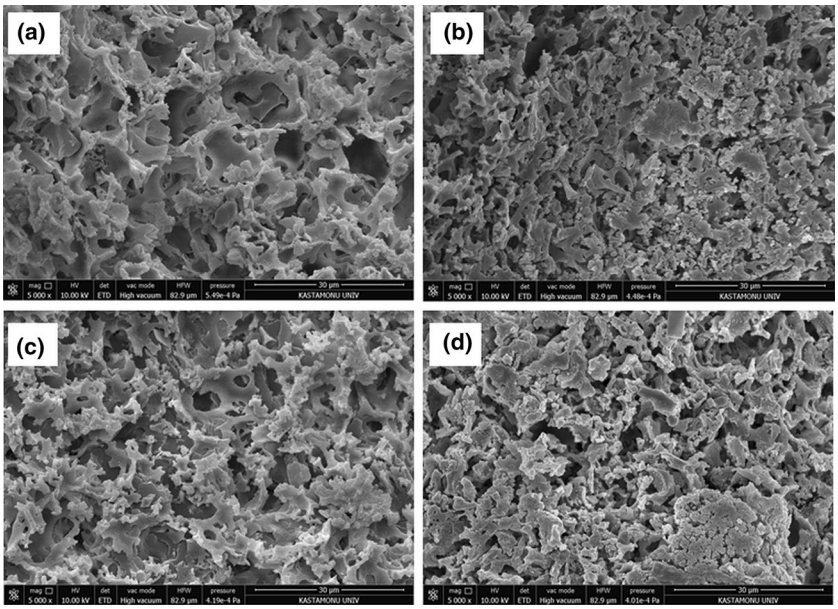

Fig. 8 SEM images of n-eicosane-based composite PCMs: MPF-EC **a**, MPF-hBN-1-EC **b**, MPF-hBN-5-EC **c** and MPF-hBN-9-EC **d**

were designed and implemented in an experimental test system, which is depicted in Fig. 10. Thus, the thermal conduction property enhancement via loading h-BN was verified. Moreover, phase transition properties of composite PCMs, which were obtained by DSC analyses, were also confirmed by using the established test system. The system was composed of a circulated bath, thermocouples, data logger and computer. As a beginning, samples measured in equivalent quantities were put in test tubes. Following that, thermocouples (K-type) were settled inside the tubes to follow up the temperature changes during the observation. Ethanol was used as the heat-transfer fluid in the circulated bath. The identical heat dissipation within the bath was obtained by a circulation pump. Initially, the temperature of the bath was fixed at 10 °C. Then, the test tubes involving the specimens were placed in the temperature-controlled bath. In both scenarios, the experiment was started when the thermal equilibrium was achieved within the bath, and the following procedures were implemented. First, the heating process was launched, and the circulated bath was heated to approximately 55 °C. Afterward, the temperature of the bath was kept constant at this temperature for 15 min, and then, the cooling step was launched. The cooling process was terminated when the bath temperature reached 10 °C again, and it was fixed at this temperature. During the test, temperature variations of the samples were measured with thermocouples, and the measurements were gathered by a data-acquisition system and saved on the computer.

Thermal behavior of the MPF and h-BN-loaded MPFs, namely MPF-hBN-1, MPF-hBN-5 and MPF-hBN-9, is demonstrated in Fig. 11. In this way, the thermal conductivity enhancements of the h-BN-loaded MPFs were observed during heating and cooling processes. According to Fig. 11, both in heating and cooling processes, MPF-hBN-9 reached firstly the target temperatures, and it was followed by MPF-hBN-5, while the MPF-hBN-1 and MPFs reached almost at the same periods. This means that the MPF-hBN-9 warms and cools faster than the other composite MPFs and also the neat MPF, due to the loading amount of h-BN (Fig. 11). Moreover, an indicator property called as the heat storage rate was calculated for each sample via dividing range of specific temperature with specific time range. Accordingly, the ranking of the samples from highest to lowest based on the thermal conduction property was determined as MPF-hBN-9 > MPF-hBN-5 > MPF-hBN-1 > MPF (Table 6). For example, the loading of 9% h-BN into the support, the heat storage rates were increased from 0,0395 to 0,0412 °C s^{-1} for heating and 0,0121 to 0,0132 °C s^{-1} for cooling processes. Hence, the percentages of increments were obtained as 4.30% and 9.09%, respectively. Examining the results of the test, it was confirmed that even a small amount of h-BN loading can obviously enhance the thermal conduction property of the composites.

In the second test, the phase transition behaviors of the obtained composite PCMs and pure PCM (EC) were investigated. Figure 12 presents the time course of temperature variations of the samples within the heating and cooling

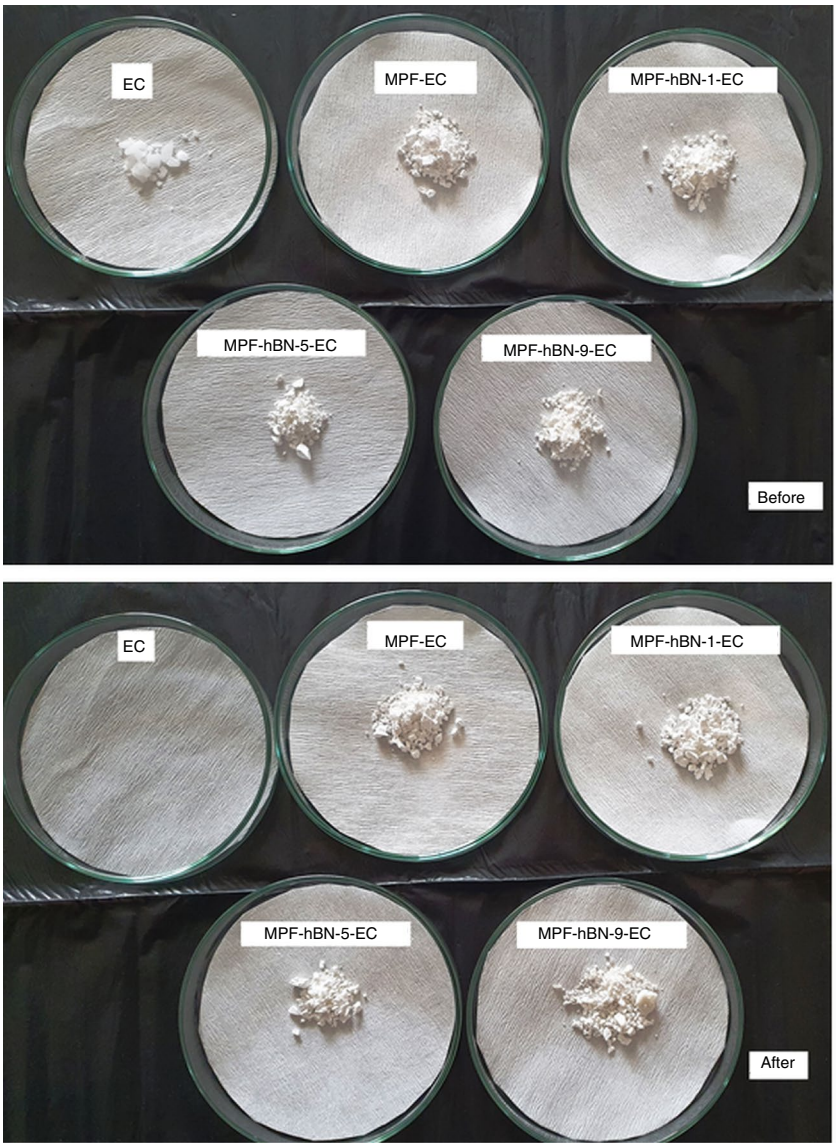

Fig. 9 The photographs of n-eicosane-based composite PCMs before and after leakage test

periods. Hence, the melting and crystallization processes of the samples were observed and compared with the obtained DSC data (Table 4). According to Fig. 12, ethanol as bath liquid was plotted as a reference material and showed neither a phase change nor a corresponding peak within the test temperatures. Moreover, the onset melting temperatures of MPF-hBN-1-EC, MPF-hBN-5-EC and MPF-hBN-9-EC were found from the DSC analyses as 34.85 ºC, 34.52 ºC and 34.39 ºC, respectively, that also observed in the heating step of the thermal behavior test (Fig. 12). On the other hand, during the cooling process, the onset crystallization temperatures of MPF-hBN-1-EC, MPF-hBN-5-EC and MPF-hBN-9-EC were seen at around 34 ºC for all composites. Consequently, the obtained results of thermal behavior test were found to be compatible with DSC analyses.

Thermal reliability of composite PCM, which has the highest h-BN loading, was investigated by thermal cycling test, and DSC curves are presented in Fig. 13.

The composite PCM (MPF-hBN-9-EC) have onset melting temperatures of 34.39 °C before cycling and 34.76 °C after 100 cycling. The onset crystallization temperatures were found to be 34.00 °C before cycling and 34.65 °C after 100 cycling. According to this result, deviations of 0.37 °C and 0.65 °C were observed in the melting and crystallization temperatures of the composite. In addition,

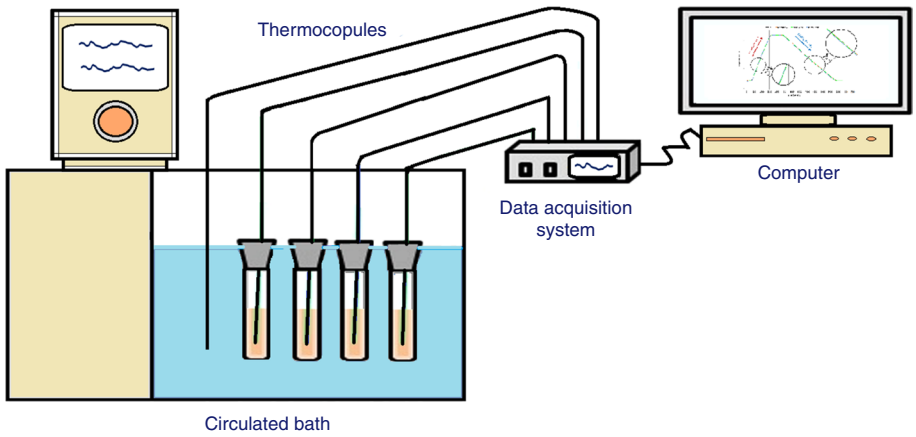

Fig. 10 Scheme of the experimental setup for the observation of thermal performance of the specimens

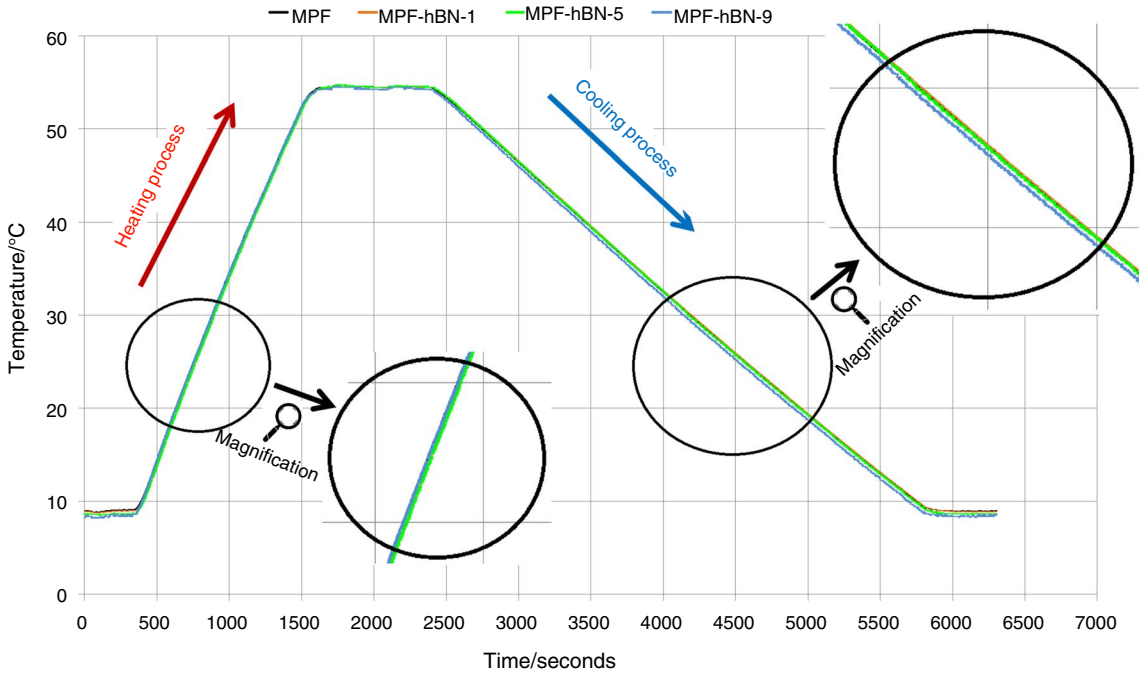

Fig. 11 Thermal behavior of the MPF, MPF-Hbn-1, MPF-Hbn-5 and MPF-Hbn-9 during heating and cooling processes

Table 6 The computed heat storage rates of the specimens during heating and cooling processes

Stage	Observation	MPF	MPF-hBN-1	MPF-hBN-5	MPF-hBN-9
Heating process	Heat storage rate /(°C s^{-1})	0,0395	0,0398	0,0405	0,0412
	Percentage of increment	–	% 0,76	% 2,53	% 4,30
Cooling process	Heat storage rate /°C s^{-1}	0,0121	0,0125	0,0129	0,0132
	Percentage of increment	–	% 3,31	% 6,61	% 9,09

the latent heat of melting/crystallization after 100 cycling was found to be 76.62 J g^{-1}/ – 69.79 J g^{-1}, which is close to the values determined as 77.10 J g^{-1}/ – 71.60 J g^{-1} before the thermal cycling test. The latent heats of melting and crystallization have variation of – 0.62 and – 2.52%, respectively, after 100th cycles, which are confirmed the thermal reliability of composite PCM.

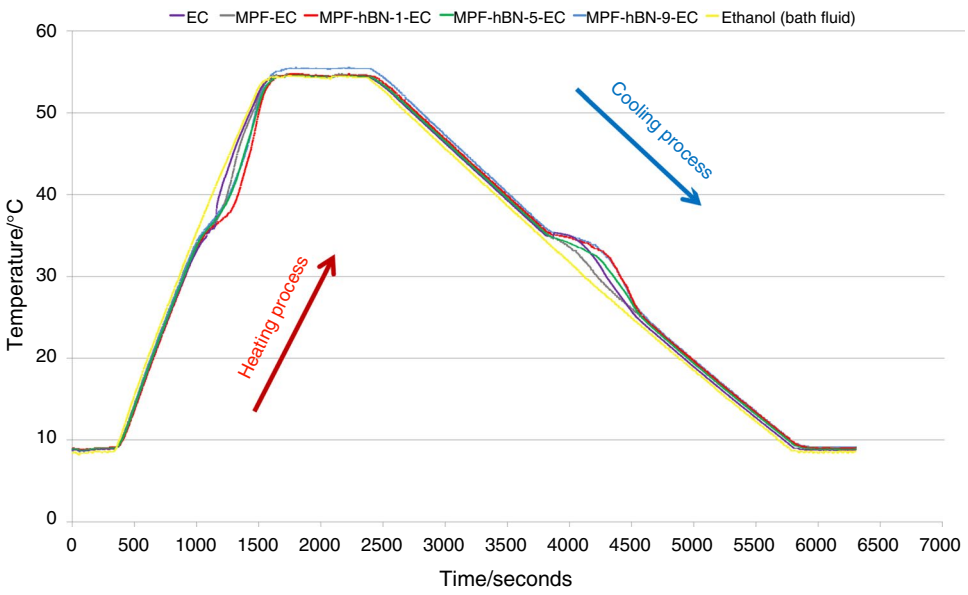

Fig. 12 The heating and cooling curves of the composite PCMs (MPF-EC, MPF-hBN-1-EC, MPF-hBN-5-EC and MPF-hBN-9-EC) and pure PCM (EC)

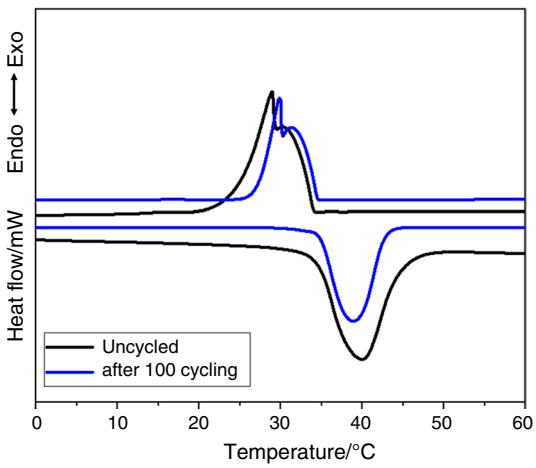

Fig. 13 DSC curves of the samples before and after thermal cycling test

Conclusions

Phase-change materials (PCMs) are smart materials that can be used in cost-effective and clean energy applications with thanks to be capable of exchanging energy. A series of new composite PCMs were prepared by using a thermally conductive material called hexagonal boron nitride (h-BN). For accomplishing this goal, first, hexagonal boron nitride (h-BN) was synthesized, second, loaded into porous polymer foams by using emulsion-templating method and third, n-eicosane, which was selected as latent heat storage material, was impregnated into the obtained macroporous polyHIPE foams (MPFs) as the support matrix. Thereby, h-BN-loaded materials (at various loadings; 0, 1, 5 and 9 mass/%) with enhanced thermal conduction properties, which were capable of thermal energy storage, were fabricated. The characterization studies of the prepared composites were performed by conducting the SEM, BET, FT-IR, TG and DSC analyses. Further;tested, and the phase-change behaviors of samples during the heating/cooling process were monitored via thermal performance tests.

The latent heat of melting of the composite PCMs with different h-BN additives (0, 1, 5 and 9 mass/%) were between 73.50 J g^{-1} and 79.00 J g^{-1}, which can be considered as a narrow range, and it was found that the composites have suitable thermal energy storage capacities and phase-change temperature for low level applications. Furthermore, based on the DSC data, EC as pure PCM has a phase transition temperature between 24.53 and 43.45 ºC, while these values for MPF-hBN-9-EC are 23.81 and 43.08 ºC. This result indicated that the incorporation of EC into the macroporous polyHIPE foams, and the loading of h-BN had a negligible little effect on the phase-change temperatures of the composite PCMs when compared to EC, the pure PCM. On the other hand, it was shown and confirmed by the applied thermal test that the addition of h-BN at 9 mass/% into the structure significantly enhanced the thermal conduction property. Namely, according to the performance tests carried out, the MPF-hBN-9-EC composite PCM reached a target temperature faster than the others both in heating and cooling processes due to its improved heat conduction property. The percentages of thermal performance enhancements of MPF-hBN-9-EC were obtained as 4.30 and 9.09%, respectively, for heating and cooling processes. According to the findings of this study, it can be safely stated based on

the relatively high latent heats and appropriate phase-change temperatures of the resulting shape-stabilized composite PCMs with different h-BN loadings that they can be used in the thermal management applications, such as cooling of electronic devices, requiring sealed properties.

Author contribution Hatice Hande MERT performed conceptualization, methodology, investigation, writing-original draft, visualization, writing-reviewing and editing. Esra BILGIN SIMSEK done conceptualization, methodology, investigation, writing-original draft and visualization. Zeynep BALTA did investigation and visualization. Mehmet Selçuk MERT performed conceptualization, methodology, investigation, writing-original draft, visualization, writing-reviewing and editing.

References

1. Teggar M, Arıcı M, Mert MS, Mousavi Ajarostaghi SS, Niyas H, Tunçbilek E, Ismail KAR, Younsi Z, Benhouia AT, Mezaache EH. A comprehensive review of micro/nano enhanced phase change materials. J Therm Anal Calorim. 2022;147:3989–4016. https://doi.org/10.1007/s10973-021-10808-0.
2. Singh P, Sharma RK, Ansu AK, Goyal R, Sarı A, Tyagi VV. A comprehensive review on development of eutectic organic phase change materials and their composites for low and medium range thermal energy storage applications. Sol Energy Mater Sol Cells. 2021;223:110955. https://doi.org/10.1016/j.solmat.2020.110955.
3. Umair MM, Zhang Y, Iqbal K, Zhang S, Tang B. Novel strategies and supporting materials applied to shape-stabilize organic phase change materials for thermal energy storage–a review. Appl Energy. 2019;235:846–73. https://doi.org/10.1016/j.apenergy.2018.11.017.
4. Do JY, Son N, Shin J, Chava RK, Joo SW, Kang M. n-eicosane-Fe_3O_4@ SiO_2@ Cu microcapsule phase change material and its improved thermal conductivity and heat transfer performance. Mater Des. 2021;198:109357. https://doi.org/10.1016/j.matdes.2020.109357.
5. Rathore PKS, Shukla SK. Enhanced thermophysical properties of organic PCM through shape stabilization for thermal energy storage in buildings: a state of the art review. Energy Build. 2021;236:110799. https://doi.org/10.1016/j.enbuild.2021.110799.
6. Huang X, Chen X, Li A, Atinafu D, Gao H, Dong W, Wang G. Shape-stabilized phase change materials based on porous supports for thermal energy storage applications. J Chem Eng. 2019;356:641–61. https://doi.org/10.1016/j.cej.2018.09.013.
7. Lin Y, Jia Y, Alva G, Fang G. Review on thermal conductivity enhancement, thermal properties and applications of phase change materials in thermal energy storage. Renew Sust Energ Rev. 2018;82(3):2730–42. https://doi.org/10.1016/j.rser.2017.10.002.
8. Qureshi ZA, Ali HM, Khushnood S. Recent advances on thermal conductivity enhancement of phase change materials for energy storage system: a review. Int J Heat Mass Transf. 2018;127:838–56. https://doi.org/10.1016/j.ijheatmasstransfer.2018.08.049.
9. Mert HH, Mert MS. Preparation and characterization of encapsulated phase change materials in presence of gamma alumina for thermal energy storage applications. Thermochim Acta. 2019;681:178382. https://doi.org/10.1016/j.tca.2019.178382.
10. Chen X, Yu H, Gao Y, Wang L, Wang G. The marriage of two-dimensional materials and phase change materials for energy storage, conversion and applications. EnergyChem. 2022;4(2):100071. https://doi.org/10.1016/j.enchem.2022.100071.
11. Shahid UB, Abdala A. A critical review of phase change material composite performance through figure-of-merit analysis: graphene vs boron nitride. Energy Storage Mater. 2021;34:365–87. https://doi.org/10.1016/j.ensm.2020.10.004.
12. Hou X, Yu Z, Chou KC. Facile synthesis of hexagonal boron nitride fibers with uniform morphology. Ceram Int. 2013;39(6):6427–31. https://doi.org/10.1016/j.ceramint.2013.01.070.
13. Huang T, Yang F, Wang T, Wang J, Li Y, Huang J, Chen M, Wu L. Ladder-structured boron nitride nanosheet skeleton in flexible polymer films for superior thermal conductivity. Appl Mater Today. 2022;26:101299. https://doi.org/10.1016/j.apmt.2021.101299.
14. Liu X, Rao Z. Interfacial thermal conductance across hexagonal boron nitride & paraffin based thermal energy storage materials. J Energy Storage. 2020;32:101860. https://doi.org/10.1016/j.est.2020.101860.
15. Chen H, Ginzburg VV, Yang J, Yang Y, Liu W, Huang Y, Du L, Chen B. Thermal conductivity of polymer-based composites: Fundamentals and applications. Prog Polym Sci. 2016;59:41–85. https://doi.org/10.1016/j.progpolymsci.2016.03.001.
16. Fang X, Fan LW, Ding Q, Yao XL, Wu YY, Hou JF, Wang X, Yu ZT, Cheng GH, Hu YC. Thermal energy storage performance of paraffin-based composite phase change materials filled with hexagonal boron nitride nanosheets. Energy Convers Manag. 2014;80:103–9. https://doi.org/10.1016/j.enconman.2014.01.016.
17. Su D, Jia Y, Alva G, Tang F, Fang G. Preparation and thermal properties of n–octadecane/stearic acid eutectic mixtures with hexagonal boron nitride as phase change materials for thermal energy storage. Energy Build. 2016;131:35–41. https://doi.org/10.1016/j.enbuild.2016.09.022.
18. Xie B, Li C, Chen J, Wang N. Exfoliated 2D hexagonal boron nitride nanosheet stabilized stearic acid as composite phase change materials for thermal energy storage. Sol Energy. 2020;204:624–34. https://doi.org/10.1016/j.solener.2020.05.004.
19. Zhang T, Xu Z, Li X, Gao G, Zhao Y. Closed-cell, phase change material-encapsulated, emulsion-templated monoliths for latent heat storage: flexibility and rapid preparation. Appl Mater Today. 2020;21:100831. https://doi.org/10.1016/j.apmt.2020.100831.
20. Puupponen S, Mikkola V, Ala-Nissila T, Seppälä A. Novel microstructured polyol–polystyrene composites for seasonal heat storage. Appl Energy. 2016;172:96–106. https://doi.org/10.1016/j.apenergy.2016.03.023.
21. Can G, Mert HH, Mert MS. Shape-stabilized n-heptadecane/polymeric foams with modified iron oxide nanoparticles for thermal energy storage. Thermochim Acta. 2022;714:179266. https://doi.org/10.1016/j.tca.2022.179266.
22. Maleki M, Ahmadi PT, Mohammadi H, Karimian H, Ahmadi R, Emrooz HBM. Photo-thermal conversion structure by infiltration of paraffin in three dimensionally interconnected porous polystyrene-carbon nanotubes (PS-CNT) polyHIPE foam. Sol Energy Mater Sol Cells. 2019;191:266–74. https://doi.org/10.1016/j.solmat.2018.11.022.
23. Döğüşcü DK, Hekimoğlu G, Sarı A. High internal phase emulsion templated-polystyrene/carbon nano fiber/hexadecanol composites phase change materials for thermal management applications. J Energy Storage. 2021;39:102674. https://doi.org/10.1016/j.est.2021.102674.
24. Doguscu DK, Hekimoglu G, Sari A. CuO nanoparticle@ polystyrene hierarchical porous foam for the effective encapsulation of octadecanol as a phase changing thermal energy storage material. Energy Fuels. 2022;36(6):3293–303. https://doi.org/10.1021/acs.energyfuels.1c04401.

25. Balta Z, Bilgin Simsek E. Understanding the structural and photocatalytic effects of incorporation of hexagonal boron nitride whiskers into ferrite type perovskites (BiFeO3, MnFeO3) for effective removal of pharmaceuticals from real wastewater. J Alloys Compd. 2022;898:162897. https://doi.org/10.1016/j.jallcom.2021.162897.
26. Sun C, Guo C, Ma X, Xu L, Qian Y. A facile route to prepare boron nitride hollow particles at 450 °C. J Cryst Growth. 2009;311(14):3682–6. https://doi.org/10.1016/j.jcrysgro.2009.05.019.
27. Mert HH, Eslek A, Mert MS, Mert EH. Preparation of Pickering-polyHIPEs from surface modified pumice stabilized high internal phase emulsions as supporting materials for lauric acid impregnation. J Appl Polym Sci. 2022;139(14):51892. https://doi.org/10.1002/app.51892.
28. Hou X, Li Q, Yang Z, Zhang Y, Zhang W, Wang JJ. Temperature–humidity dual regulation of a single-core–double-shell microcapsule fabricated by electrostatic-assembly and chemical precipitation. RSC Adv. 2020;10(44):26494–503. https://doi.org/10.1039/D0RA03554H.
29. Li B, Liu T, Hu L, Wang Y, Gao L. Fabrication and properties of microencapsulated paraffin@ SiO_2 phase change composite for thermal energy storage. ACS Sustain Chem Eng. 2013;1(3):374–80. https://doi.org/10.1021/sc300082m.